ARTICLE

Numerical Investigation on 1,3-Butadiene/Propyne Co-pyrolysis and Insight into Synergistic Effect on Aromatic Hydrocarbon Formation

Tian-yu Li[a], Jia-biao Zou[b], Yan Zhang[b], Chuang-chuang Cao[a], Wei Li[a], Wen-hao Yuan[b*]

a. National Synchrotron Radiation Laboratory, University of Science and Technology of China, Hefei 230029, China

b. Key Laboratory for Power Machinery and Engineering of MOE, Shanghai Jiao Tong University, Shanghai 200240, China

(Dated: Received on March 12, 2017; Accepted on May 10, 2017)

A numerical investigation on the co-pyrolysis of 1,3-butadiene and propyne is performed to explore the synergistic effect between fuel components on aromatic hydrocarbon formation. A detailed kinetic model of 1,3-butadiene/propyne co-pyrolysis with the sub-mechanism of aromatic hydrocarbon formation is developed and validated on previous 1,3-butadiene and propyne pyrolysis experiments. The model is able to reproduce both the single component pyrolysis and the co-pyrolysis experiments, as well as the synergistic effect between 1,3-butadiene and propyne on the formation of a series of aromatic hydrocarbons. Based on the rate of production and sensitivity analyses, key reaction pathways in the fuel decomposition and aromatic hydrocarbon formation processes are revealed and insight into the synergistic effect on aromatic hydrocarbon formation is also achieved. The synergistic effect results from the interaction between 1,3-butadiene and propyne. The easily happened chain initiation in the 1,3-butadiene decomposition provides an abundant radical pool for propyne to undergo the H-atom abstraction and produce propargyl radical which plays key roles in the formation of aromatic hydrocarbons. Besides, the 1,3-butadiene/propyne co-pyrolysis includes high concentration levels of C3 and C4 precursors simultaneously, which stimulates the formation of key aromatic hydrocarbons such as toluene and naphthalene.

Key words: 1,3-Butadiene, Propyne, Kinetic model, Synergistic effect, Aromatic hydrocarbon formation

I. INTRODUCTION

Aromatic hydrocarbons and soot are important combustion pollutants due to their carcinogenicity and mutagenicity [1–5]. Consequently their formation mechanisms in combustion have attracted special attentions for a long time [1, 6–10]. In general, the formation of soot is a complex process with several major steps [1], including the formation of first benzene ring via the combination of small C1−C5 unsaturated molecules, the formation and growth of polycyclic aromatic hydrocarbons (PAHs), the nascent soot formation, the growth of soot, and the formation of mature soot. The formation of the first benzene ring is recognized as the rate-controlling step in the formation of PAHs and soot [1]. A series of experimental studies found that many mixtures containing two or more components (at a given ratio) would generate more aromatic hydrocarbons and soot in comparison with any single component under the same condition, such as the mixtures of methane/ethylene [11, 12], ethylene/propane [13, 14], 1,3-butadiene/propyne [15], toluene/*n*-heptane [16], and so on. This phenomenon is defined as the synergistic effect between fuel components on the formation processes of aromatic hydrocarbons and soot, which shows not only the interaction of different fuel decomposition products on soot formation, but also the diversity of critical pathways of benzene and PAHs formation. Due to the complex components of transportation fuels, synergistic effect is one of the crucial factors influencing soot emissions [1]. Compared with the experimental study of synergistic effect, the models and numerical research are rather limited, which leads to the lack of the understanding of the cause of synergistic effect. This lack not only affects the understanding of aromatics and soot formation mechanism but also makes the control of soot emissions difficult consequently.

Among the mixtures with synergistic effect, the 1,3-butadiene/propyne mixture is a typical one since it presents a combination of odd C-atoms and even C-atoms. The synergistic effect between the two fuels was recently reported by Poddar *et al.* [15] in the aromatic hydrocarbon formation process under pyrolytic conditions. They found that the production of aromatic hy-

*Author to whom correspondence should be addressed. E-mail: yuanwh@sjtu.edu.cn, Tel.: +86-21-34204115

drocarbons in the 1,3-butadiene/propyneco-pyrolysis experiments was much higher than that in any single component pyrolysis experiments performed by the same group [15, 17, 18]. Similarly to other fuel mixtures with synergistic effect, there is no analysis work on this system to explore the reason leading to the synergistic effect between 1,3-butadiene and propyne since there is no kinetic model of 1,3-butadiene/propyne co-pyrolysis.

In this work, a kinetic model of 1,3-butadiene/propyne co-pyrolysis is developed with consideration of both the fuel decomposition sub-mechanisms and the sub-mechanism of aromatic hydrocarbon formation. Validation on previous 1,3-butadiene and propyne pyrolysis experiments is performed to ensure the reliability of the model. Numerical simulation is carried out for the co-pyrolysis experiment reported by Poddar *et al.* [15], while the rate of production (ROP) and sensitivity analyses are performed to reveal the key formation pathways of aromatic hydrocarbons. This work provides insight into the synergistic effect between fuel components.

II. KINETIC MODEL AND NUMERICAL SIMULATION METHOD

The development of the kinetic model of 1,3-butadiene/propyne co-pyrolysis originates from our recent aromatic hydrocarbon models [10, 19–22]. The sub-mechanism of 1,3-butadiene developed in this work mainly contains the isomerization, unimolecular decomposition, addition, H-atom abstraction reactions. The sub-mechanism of propyne mainly includes the isomerization, addition and H-atom abstraction reactions. The sub-mechanism of aromatic hydrocarbon formation includes two sets of reactions, *i.e.* formation reactions of monocyclic aromatic hydrocarbons and formation/growth reactions of PAHs. In the present model, the formation reactions of benzene mainly include the C4+C2 and C3+C3 pathways. The C4+C2 pathway which belongs to the even C-atom mechanism include the addition of acetylene to vinyl acetylene and 1,3-butadienyl radical, and the rate constants experimentally investigated by Chanmugathas *et al.* [23] and theoretically investigated by Miller *et al.* [24] are adopted in this model, respectively. The C3+C3 pathway which belongs to the odd C-atom mechanism include the self-combination of propargyl radical and the reactions of propargyl radical with propyne (pC_3H_4) and allene (aC_3H_4). Miller *et al.* [24] investigated the self-combination of propargyl radical theoretically and their recommended rate constant is used. The reactions of propargyl radical with propyne and allene are taken from the model of D'Anna *et al.* [25]. The formation pathways of toluene mainly include the C3+C4 and C1+C6 pathways [26]. As for the formation pathway of indene, the rate constant of addition of acetylene to benzyl radical is adopted from the theoretical investigation of Vereecken *et al.* [27]. The rate constant of addition of propargyl radical to benzene is estimated in this work, and the rate constant of reaction between cyclopentadienyl radical and cyclopentadiene is adopted from the theoretical calculation result of Cavallotti *et al.* [28]. The formation pathway of naphthalene includes the hydrogen-abstraction/carbon-addition (HACA) pathways [29, 30] and the reaction between vinylacetylene and phenyl radical with the rate constant recommended in the model of Blanquart *et al.* [31]. The reaction of propargyl radical with benzyl radical forms methylindenyl and H-atom and 1-methyleneindan-2-yl radical decomposes to naphthalene and H-atom subsequently. The rate constant of the two reactions are adopted from the theoretical investigation of Matsugi *et al.* [32]. The presentsub-mechanism of aromatic hydrocarbons has been validated from a lot of experimental data [10, 19–22]. The final model consists of 278 species and 1705 reactions.

The thermodynamic data are mainly taken from the thermodynamics database [33] or our previous models [10, 19–22], while the transport data are taken from the Chemkin transport database [34] or our previous models [10, 19–22]. For the shock tube pyrolysis experiments, the simulation is performed with the closed homogeneous batch reactor module in the Chemkin-Pro software [35]. For the flow reactor pyrolysis experiments, the simulation is performed with the plug flow reactor module in the Chemkin-Pro software [35]. In the flow reactor experiments, Thomas *et al.* [17] and Poddar *et al.* [15, 18] only provided the information of residence time which is 0.3 s. Therefore in the simulation, the inlet axial velocity is set as 30 cm/s, while the starting and ending axial positions are set as 0 and 9 cm, respectively. As a result, the residence time in the simulation is also 0.3 s which is consistent with the experimental condition.

III. RESULTS AND DISCUSSION

A. Model validation on single component pyrolysis

The present model is validated on the shock tube pyrolysis data of 1,3-butadiene and propyne reported by Hidaka *et al.* [36, 37], the flow reactor pyrolysis data of 1,3-butadiene by Thomas *et al.* [17], and the flow reactor pyrolysis data of propyne by Poddar *et al.* [18]. The 1,3-butadiene shock tube pyrolysis was performed for 6% 1,3-butadiene and 94% argon at 50 Torr [37], while the propyne shock tube pyrolysis was performed for 4% propyne and 96% argon at 1.7−2.6 atm [36]. The two flow reactor pyrolysis experiments [17, 18] are actually the single component experiments for the 1,3-butadiene/propyne co-pyrolysis experiment reported by the same group [15]. The experimental conditions of three flow reactor pyrolysis experiments [15, 17, 18] are listed in Table I with PY-C4, PY-C3, and CO-PY de-

DOI:10.1063/1674-0068/30/cjcp1703031

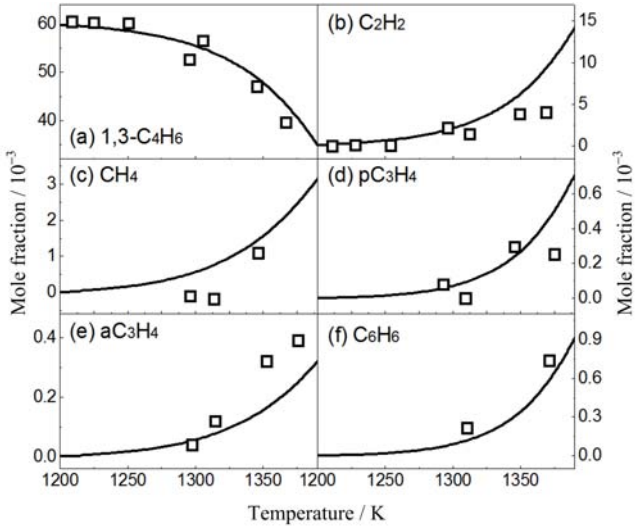

FIG. 1 Simulated results (lines) of (a) 1,3-butadiene, (b) acetylene, (c) methane, (d) propyne, (e) allene, and (f) benzene in the shock tube pyrolysis of 1,3-butadiene compared with the experimental data (symbols) reported by Hidaka *et al.* [37].

TABLE I Conditions of three flow reactor pyrolysis experiments [15, 17, 18]. P=1 atm, t=0.3 s.

	C_4H_6	pC_3H_4	N_2
PY-C4	0.1320%	0	99.868%
PY-C3	0	0.1155%	99.8845%
CO-PY	0.1400%	0.1400%	99.7200%

noting the 1,3-butadiene pyrolysis, propyne pyrolysis and co-pyrolysis experiments.

The simulated results of the shock tube pyrolysis of 1,3-butadiene and propyne are compared with the experimental results [36, 37] in FIG. 1 and 2, respectively. From the two figures it can be observed that the present model has a generally good performance in capturing the trends of fuel decomposition and product formations for both 1,3-butadiene and propyne.

FIG. 3 and 4 show the comparison of the simulated results and experimental data for the PY-C4 case reported by Thomas *et al.* [17] and the PY-C3 case reported by Poddar *et al.* [18], respectively. In order to be consistent with the work of Thomas *et al.* [17] and Poddar *et al.* [18], the term "%Fed C as C in given products", *i.e.* the percentage in the total fed carbon for given products, is adopted here instead of the conventionally used "mole fraction", and this can eliminate the influence of C-atom numbers in different species.

As shown in FIG. 3 and 4, the present model well predicts the decomposition of fuels and the formation of products in both PY-C4 and PY-C3 experiments. For the PY-C4 case, the ROP analysis is performed at 1173 K when the products have already been abundantly produced. According to the ROP analysis, 51%

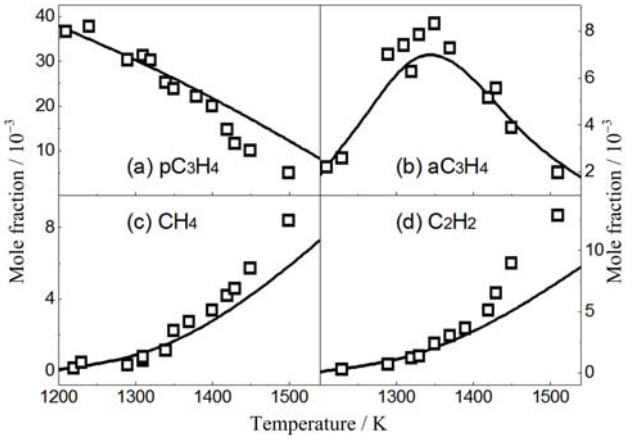

FIG. 2 Simulated results (lines) of (a) propyne, (b) allene, (c) methane and (d) acetylene in the shock tube pyrolysis of propyne compared with the experimental data (symbols) reported by Hidaka *et al.* [36].

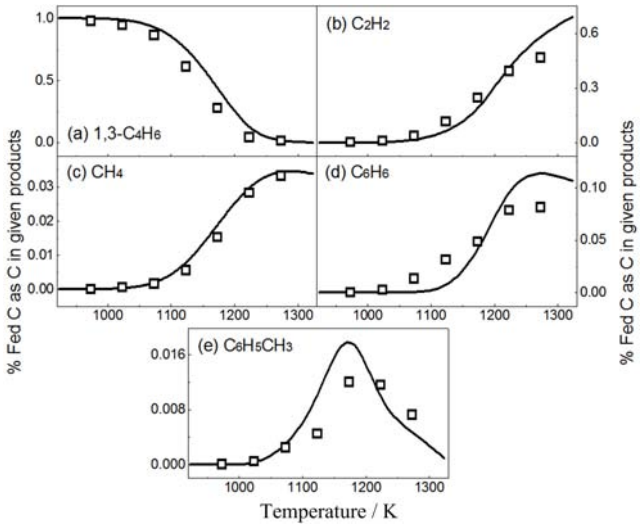

FIG. 3 Simulated results (lines) of (a) 1,3-butadiene, (b) acetylene, (c) methane, (d) benzene, and (e) toluene in the PY-C4 case compared with experimental data (symbols) reported by Thomas *et al.* [17].

of 1,3-butadiene decomposes to ethylene and vinyl radical via the H-atom attack reaction (Eq.(1)), while the β-C-H scission of vinyl radical leads to the formation of acetylene. 10% of 1,3-butadiene decomposes to ethylene and acetylene via the unimolecular decomposition reaction (Eq.(2)), which contributes 13% to the production of acetylene. 8% of 1,3-butadiene is consumed via the H-atom abstraction reaction bymethyl radical (Eq.(3)) to produce 1,3-butadien-2-yl (iC_4H_5) radical and methane, which dominates the formation of both products. iC_4H_5 radical mainly suffers the β-C-H scission reaction to produce vinylacetylene (Eq.(4)), which is also the dominant formation pathway of vinyl acetylene. Besides, 9% of 1,3-butadiene can be isomerized

DOI:10.1063/1674-0068/30/cjcp1703031

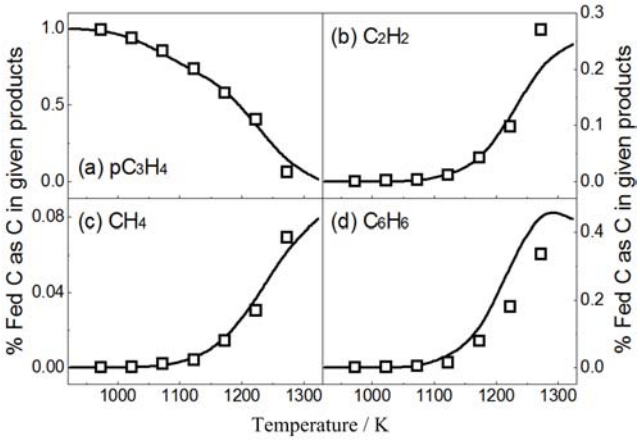

FIG. 4 Simulated results (lines) of (a) propyne, (b) acetylene, (c) methane, and (d) benzene in the PY-C3 case compared with the experimental data (symbols) reported by Poddar *et al.* [18].

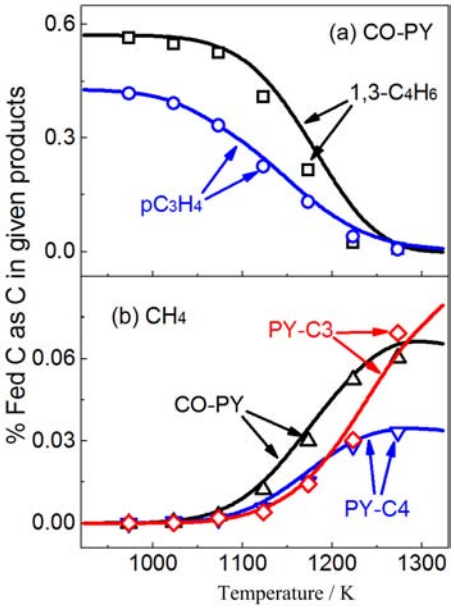

FIG. 5 (a) Simulated results (lines) of 1,3-butadiene and propyne in the CO-PY case compared with the experimental data (symbols) reported by Poddar *et al.* [15]. (b) Simulated results (lines) of methane in the CO-PY, PY-C4, and PY-C3 cases compared with the experimental data (symbols) reported by Poddar *et al.* [15], Thomas *et al.* [17], and Poddar *et al.* [18].

to 1,2-butadiene via Eq.(5). 1,2-Butadiene can further decompose to propargyl radical and methyl radical through Eq.(6), which is the most important chain initiation reaction in the pyrolysis of 1,3-butadiene. The simulated results of two aromatic products in the PY-C4 case, *i.e.* benzene and toluene, are also presented in FIG. 3. The main pathway of toluene formation is the addition reaction between propargyl radical and 1,3-butadiene. The benzene formation is controlled by several pathways, including the isomerization of fulvene, the decomposition of toluene, self-combination of propargyl radical, and so on.

$$1,3\text{-}C_4H_6 + H = C_2H_4 + C_2H_3 \quad (1)$$
$$1,3\text{-}C_4H_6 = C_2H_4 + C_2H_2 \quad (2)$$
$$1,3\text{-}C_4H_6 + CH_3 = iC_4H_5 + CH_4 \quad (3)$$
$$C_4H_4 + H = iC_4H_5 \quad (4)$$
$$1,3\text{-}C_4H_6 = 1,2\text{-}C_4H_6 \quad (5)$$
$$1,2\text{-}C_4H_6 = C_3H_3 + CH_3 \quad (6)$$

For the PY-C3 case, the ROP analysis is also performed at 1173 K when the products have already abundantly produced. The ROP analysis shows that 59% of propyne forms allene via the isomerization reaction (Eq.(7)), which contributes 98% to the production of allene. It is noticed that the unimolecular decomposition of allene producing propargyl radical and H atom is the main chain initiation reaction in the PY-C3 case, however this reaction is much more difficult to happen than Eq.(6) in the PY-C4 case. Therefore the propyne pyrolysis is less abundant with free radicals compared to the 1,3-butadiene pyrolysis. The H-atom attack reaction (Eq.(8)) consumes 17% of propyne to form methyl radical and acetylene, which dominates the formation of acetylene in the PY-C3 case. Only 25% of the generated methyl radical forms ethane via the self-combination reaction, while 32% and 28% of methyl radical is consumed via the methyl radical attack reactions on propyne and allene (Eq.(9) and Eq.(10)), respectively. Propargyl radical and methane can be produced from Eq.(9) and Eq.(10), which contribute 98% to the production of methane and 63% to the production of propargyl radical. Different from the PY-C4 case, the reactions of propargyl radical with propyne and allene contribute 97% to the formation of benzene in the PY-C3 case.

$$pC_3H_4 = aC_3H_4 \quad (7)$$
$$C_2H_2 + CH_3 = pC_3H_4 + H \quad (8)$$
$$pC_3H_4 + CH_3 = C_3H_3 + CH_4 \quad (9)$$
$$aC_3H_4 + CH_3 = C_3H_3 + CH_4 \quad (10)$$

B. Analysis of synergistic effect in co-pyrolysis

As shown in FIG. 5−7, the present model well captures the decomposition of the two fed fuels and the formation of methane, ethylene, acetylene, benzene, and toluene in the CO-PY case. For the two aromatic species benzene and toluene, the synergistic effect between 1,3-butadiene and propyne on their formation is investigated. Similar to Poddar *et al.* [15], the weighted sum for a specific species is calculated from its yield values in the PY-C4 and PY-C3 cases at the same tem-

DOI:10.1063/1674-0068/30/cjcp1703031

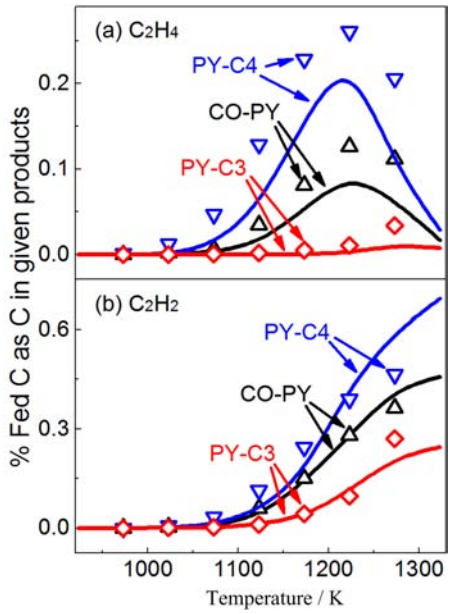

FIG. 6 Simulated results (lines) of (a) ethylene and (b) acetylene in the CO-PY, PY-C4 and PY-C3 cases compared with the experimental data (symbols) reported by Poddar *et al.* [15], Thomas *et al.* [17], and Poddar *et al.* [18].

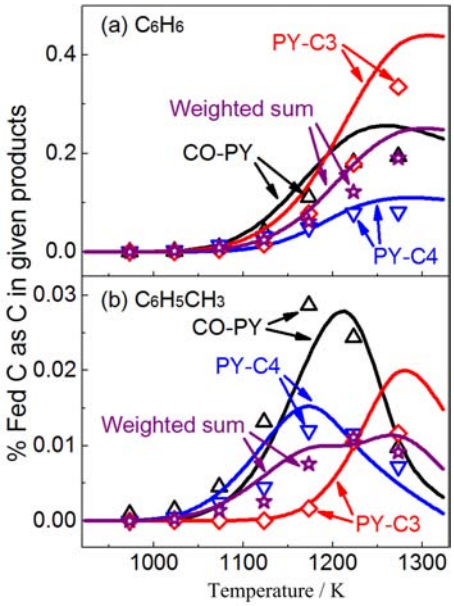

FIG. 7 Simulated results (lines) of (a) benzene and (b) toluene in the CO-PY, PY-C4 and PY-C3 cases compared with the experimental data (symbols) reported by Poddar *et al.* [15], Thomas *et al.* [17], and Poddar *et al.* [18]. The hollow stars and corresponding line in each figure represents the simluated and experimental weighted sum values calculated from Eq.(1).

perature:

$$\text{Weighted sum} = 0.571Y_{C4} + 0.429Y_{C3}$$

where 0.429 and 0.571 are the fractions of propyne and 1,3-butadiene in the total fed carbon in the CO-PY case, respectively, while Y_{C4} and Y_{C3} are the yield values from the PY-C3 and PY-C4 cases, respectively. Thus the weighted sum denotes the production of a specific species in the CO-PY case if there is no synergistic effect or other interactions between 1,3-butadiene and propyne. The main reaction network in the CO-PY case is presented in FIG. 8.

In the CO-PY case, the ROP analysis is performed at 1173 K when the fuels are consumed and the products are produced abundantly. The ROP analysis shows that 29% of 1,3-butadiene decomposes to ethylene and vinyl radical via the H-atom attack reaction (Eq.(1)), while almost all vinyl radical decomposes to acetylene and H atom. 19% of 1,3-butadiene in the CO-PY case is consumed to produce iC_4H_5 radical via the H-atom abstraction reaction by methyl radical (Eq.(3)). iC_4H_5 radical further decomposes to vinyl acetylene and H atom via the unimolecular decomposition reaction (Eq.(4)), which contributes 83% to the production of vinyl acetylene. 12% of 1,3-butadiene forms 1,2-butadiene via the isomerization reaction, and almost all 1,2-butadiene decomposes to propargyl radical and methyl radical subsequently, which contributes 33% to the production of propargyl radical. For the consumption of the other fuelpropyne, the isomerization reaction Eq.(7) only contributes 27% to the consumption of

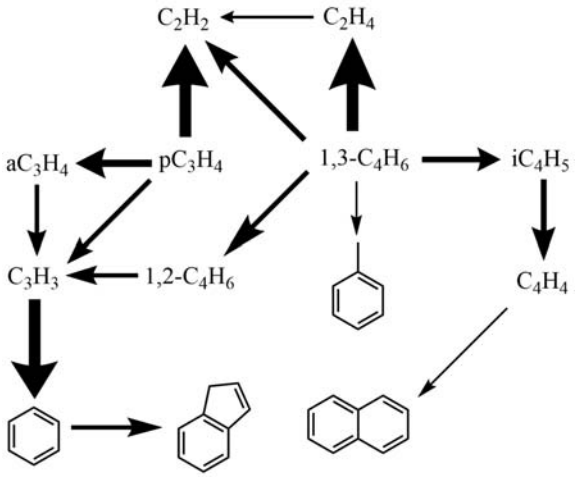

FIG. 8 Main reaction network in the CO-PY case. The arrow thickness is proportional to the carbon flux of the corresponding reaction pathway.

propyne in the CO-PY case, instead of 60% in the PY-C3 case. The H-atom attack reaction Eq.(8) becomes the most important consumption pathway of propyne with a contribution of 38%. The reason that Eq.(8) becomes more important than Eq.(7) in the CO-PY case is that the 1,3-butadiene pyrolysis system is more abundant in radicals compared with the propyne pyrolysis system, especially for H atom, according to the discussion above. This reveals the interaction between

DOI:10.1063/1674-0068/30/cjcp1703031

1,3-butadiene and propyne in the fuel decomposition processes.

As the simplest aromatic hydrocarbon, benzene has attracted great attention due to its important role in soot formation [1]. As shown in FIG. 7(a), the concentration level of benzene in the CO-PY case is much higher than that in the PY-C4 case and comparable to that in the PY-C3 case. As a result, the yield of benzene in the CO-PY case is higher than the weighted sum of those in the PY-C4 and PY-C3 cases, demonstrating the synergistic effect between 1,3-butadiene and propyne on the formation of benzene. This phenomenon can be analyzed using the ROP analysis, together with the sensitivity analysis of benzene and propargyl radical at 1173 K (FIG. 9). The ROP analysis indicates that benzene is dominantly produced from the addition reaction of propargyl radical to propyne (Eq.(11), 57%) andallene (Eq.(12), 17%) in the CO-PY case due to the high concentration levels of propyne and allene.

According to the sensitivity analysis in FIG. 9, the isomerization reaction of 1,3-butadiene to 1,2-butadiene (Eq.(5)) has the maximum positive sensitivity coefficient to the formation of both benzene and propargyl radical in the CO-PY case. This reveals the interaction between 1,3-butadiene and propyne in the formation of benzene. In the PY-C4 case, both propyne and allene can hardly be produced [17], thus the main formation pathway of benzene is only the self-combination of propargyl radical, leading to a low concentration level of benzene. In the PY-C3 case, allene is greatly produced from the isomerization of propyne and propargyl radical can be produced from the H-atom abstraction reactions of propyne, and allene, leading to a high concentration level of benzene. But it is recognized the production of propargyl radical in the PY-C3 case is not very effective due to the lack of free radicals. In the CO-PY case, the radical pool is more abundant than the PY-C3 case due to the effective chain initiation reaction sequence (Eq.(5) and Eq.(6)), and propargyl radical can be readily produced from Eq.(6) and the H-atom abstraction reactions of propyne and allene. As a result, the synergistic effect on the formation benzene can be observed in the CO-PY case.

$$\mathrm{pC_3H_4 + C_3H_3 = C_6H_6 + H} \quad (11)$$

$$\mathrm{aC_3H_4 + C_3H_3 = C_6H_6 + H} \quad (12)$$

As shown in FIG. 7(b), the yield of toluene in the CO-PY case is much higher than those in the PY-C4 and PY-C3 cases, as well as the weighted sum, indicating a great synergistic effect between 1,3-butadiene and propyne on the formation of toluene. ROP and sensitivity analyses are also performed to investigate the origin of this synergistic effect. The ROP analysis shows that toluene is dominantly produced from the effective pathway of propargyl radical+1,3-butadiene (Eq.(13)) in the PY-C4 and CO-PY cases, while the formation of toluene in the PY-C3 case has to rely on the addition

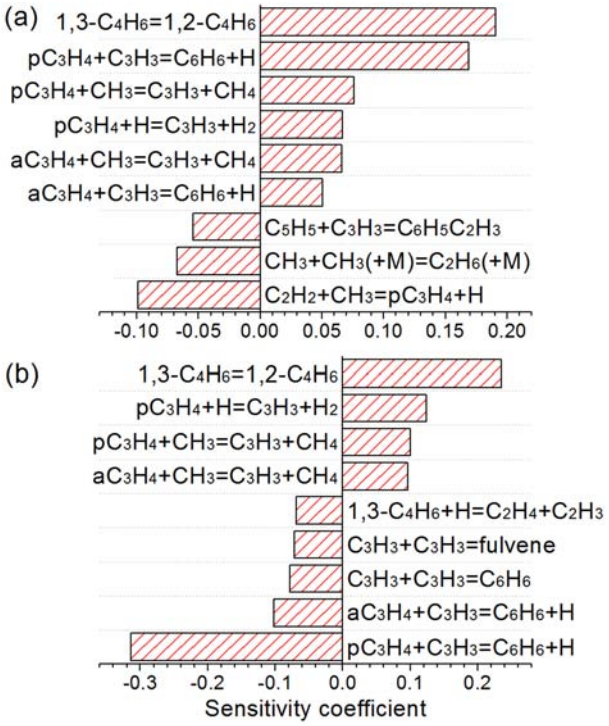

FIG. 9 Sensitivity analyses of (a) benzene and (b) propargyl radical in the CO-PY case.

of methyl radical to benzene (Eq.(14), 97%) since only negligible 1,3-butadiene can be produced [18]. The sensitivity analysis of toluene at 1173 K for the CO-PY case (FIG. 10) shows that reactions producing propargyl radical all have positive sensitivity coefficient, indicating the importance of propargyl radical to the formation of toluene. As discussed above, the production of propargyl radical is stimulated in the CO-PY cases due to the interaction of 1,3-butadiene and propyne, leading to the synergistic effect on the formation of toluene through the typical C3+C4 pathway. On the other hand, the origin of toluene from 1,3-butadiene and propargyl radical in the PY-C4 and CO-PY cases makes it be formed at much earlier stage (∼1050 K) than that (∼1150 K) in PY-C3 cases.

$$\mathrm{C_3H_3 + 1{,}3\text{-}C_4H_6 = C_6H_5CH_3 + H} \quad (13)$$

$$\mathrm{C_6H_5CH_3 + H = C_6H_6 + CH_3} \quad (14)$$

It is concluded that the reactions involving propargyl radicals play crucial roles in the synergistic effects between 1,3-butadiene and propyne on the formation of benzene and toluene. However in the experimental work of Poddar *et al.* [15, 18] and Thomas *et al.* [17], Free radicals were not able to be detected like propargyl radical due to the limitation of gas chromatography used in their work [1]. Novel diagnostic methods such as synchrotron vacuum ultraviolet photoionization mass spectrometry [2, 38–40] can detect these crucial reactive intermediates and will benefit the experimental investigations on synergistic effect.

DOI:10.1063/1674-0068/30/cjcp1703031

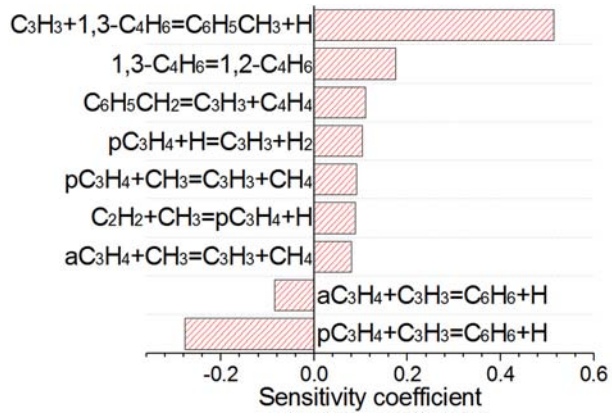

FIG. 10 Sensitivity analysis of toluene in the CO-PY case.

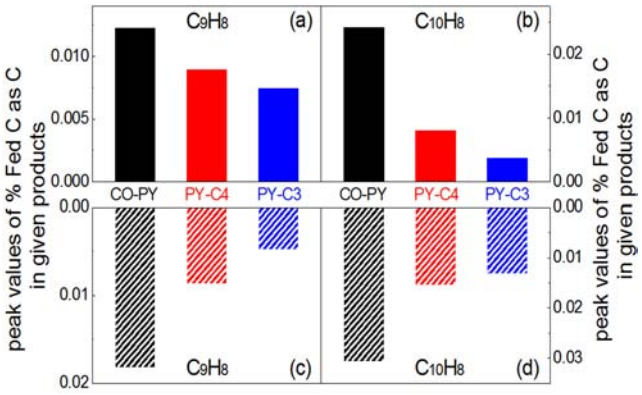

FIG. 11 Simulated results (solid columns) of (a) indene and (b) naphthalene in the CO-PY, PY-C4, and PY-C3 cases compared with the experimental data (slash columns) of (c) indene and (d) naphthalene reported by Poddar *et al.* [15], Thomas *et al.* [17] and Poddar *et al.* [18].

As the simplest PAHs, indene and naphthalene are two key species in the formation of growth processes of PAHs. FIG. 11 shows the simulated peak values of the two PAHs in the three pyrolysis cases together with the experimental data [15, 17, 18]. As observed from the experimental and simulated results, both the two PAHs have the highest yields in the CO-PY cases, indicating the synergistic effects between 1,3-butadiene and propyne on their formation. The synergistic effect on the formation of indene is mainly caused by the enhanced formation of indene through the addition of propargyl radical to benzene (Eq.(15)) in the CO-PY case due to the stimulated production of propargyl radical and benzene. The main reason for the synergistic effect on the formation of naphthalene is the reaction between phenyl radical and vinyl acetylene (Eq.(16)). This reaction is only important in the CO-PY case since the PY-C4 case produces less phenyl radical and the PY-C3 case lacks of vinyl acetylene.

$$C_6H_6 + C_3H_3 = C_9H_8 + H \quad (15)$$

$$C_6H_5 + C_4H_4 = C_{10}H_8 + H \quad (16)$$

IV. CONCLUSIONS

A detailed kinetic model of 1,3-butadiene/propyne co-pyrolysis with the sub-mechanism of aromatic hydrocarbon formation is developed. The simulated yield profiles of fuels, decomposition products and several aromatic hydrocarbons capture the experimental data of single component pyrolysis and co-pyrolysis well. The ROP and sensitivity analyses are performed to understand the key reaction pathways in the fuel decomposition and aromatic hydrocarbon formation processes which provide insight into the synergistic effects between 1,3-butadiene and propyne on aromatic hydrocarbon formation. 1,3-Butadiene is mainly consumed by the H-atom attack reaction to form ethylene and vinyl radical, while the unimolecular decomposition of its isomerization product 1,2-butadiene to propargyl radical and methyl radical is the most important chain initiation pathway. Propyne is mainly consumed via the isomerization reaction to form allene, the H-atom attack reaction to form acetylene and methyl radical, and the H-atom abstraction reactions to form propargyl radical. It is notable that in the PY-C3 case the last two reactions are suppressed due to the lack of free radicals. The synergistic effect on the formation of benzene, toluene, indene and naphthalene is concluded to result from the interaction between 1,3-butadiene and propyne. On one hand, the easily happened chain initiation in the 1,3-butadiene decomposition provides an abundant radical pool for propyne to undergo the H-atom abstraction reaction and produce propargyl radical which plays a key role in the formation of benzene, toluene and indene. On the other hand, the 1,3-butadiene/propyne co-pyrolysis includes high concentration levels of C3 and C4 precursors simultaneously, which stimulates the formation of key aromatic hydrocarbons such as toluene and naphthalene greatly.

V. ACKNOWLEDGMENTS

This work is supported by the National Natural Science Foundation of China (No.51476155, No.51622605, No.91541201), the National Key Scientific Instruments and Equipment Development Program of China (No.2012YQ22011305), the National Postdoctoral Program for Innovative Talents (No.BX201600100), and China Postdoctoral Science Foundation (No.2016M600312).

[1] C. S. McEnally, L. D. Pfefferle, B. Atakan, and K. Kohse-Höinghaus, Prog. Energy Combust. Sci. **32**, 247 (2006).

[2] F. Qi, R. Yang, B. Yang, C. Q. Huang, L. X. Wei, J. Wang, L. S. Sheng, and Y. W. Zhang, Rev. Sci. Instrum. **77**, 084101 (2006).
[3] B. Yang, Y. Y. Li, L. X. Wei, C. Q. Huang, J. Wang, Z. Y. Tian, R. Yang, L. S. Sheng, Y. W. Zhang, and F. Qi, Proc. Combust. Inst. **31**, 555 (2007).
[4] Y. Y. Li, L. D. Zhang, Z. Y. Tian, T. Yuan, J. Wang, B. Yang, and F. Qi, Energy Fuels **23**, 1473 (2009).
[5] Y. Y. Li, L. D. Zhang, Z. Y. Tian, T. Yuan, K. W. Zhang, B. Yang, and F. Qi, Proc. Combust. Inst. **32**, 1293 (2009).
[6] H. Richter and J. B. Howard, Phys. Chem. Chem. Phys. **4**, 2038 (2002).
[7] L. D. Zhang, J. H. Cai, T. C. Zhang, and F. Qi, Combust. Flame **157**, 1686 (2010).
[8] Y. Y. Li, J. H. Cai, L. D. Zhang, T. Yuan, K. W. Zhang, and F. Qi, Proc. Combust. Inst. **33**, 593 (2011).
[9] Y. Y. Li, L. D. Zhang, Z. D. Wang, L. L. Ye, J. H. Cai, Z. J. Cheng, and F. Qi, Proc. Combust. Inst. **34**, 1739 (2013).
[10] W. H. Yuan, Y. Y. Li, P. Dagaut, J. Z. Yang, and F. Qi, Combust. Flame **162**, 3 (2015).
[11] J. F. Roesler, S. Martinot, C. S. McEnally, L. D. Pfefferle, J. L. Delfau, and C. Vovelle, Combust. Flame **134**, 249 (2003).
[12] S. Trottier, H. Guo, G. J. Smallwood, and M. R. Johnson, Proc. Combust. Flame **31**, 611 (2007).
[13] J. Y. Hwang, S. H. Chung, and W. Lee, Proc. Combust. Flame **27**, 1531 (1998).
[14] J. Y. Hwang, W. Lee, H. G. Kang, and S. H. Chung, Combust. Flame **114**, 370 (1998).
[15] N. B. Poddar, S. Thomas, and M. J. Wornat, Proc. Combust. Inst. **34**, 1775 (2013).
[16] B. C. Choi, S. K. Choi, and S. H. Chung, Proc. Combust. Inst. **33**, 609 (2011).
[17] S. Thomas and M. J. Wornat, Proc. Combust. Inst. **32**, 615 (2009).
[18] N. B. Poddar, S. Thomas, and M. J. Wornat, Proc. Combust. Inst. **33**, 541 (2011).
[19] H. F. Jin, A. Frassoldati, Y. Z. Wang, X. Y. Zhang, M. R. Zeng, Y. Y. Li, F. Qi, A. Cuoci, and T. Faravelli, Combust. Flame **162**, 1692 (2015).
[20] W. H. Yuan, Y. Y. Li, P. Dagaut, J. Z. Yang, and F. Qi, Combust. Flame **162**, 22 (2015).
[21] H. F. Jin, J. H. Cai, G. Q. Wang, Y. Z. Wang, Y. Y. Li, J. Z. Yang, Z. J. Cheng, W. H. Yuan, and F. Qi, Combust. Flame **169**, 154 (2016).
[22] W. H. Yuan, Y. Y. Li, G. Pengloan, C. Togbé, P. Dagaut, and F. Qi, Combust. Flame **166**, 255 (2016).
[23] C. Chanmugathas and J. Heicklen, Int. J. Chem. Kinet. **18**, 701 (1986).
[24] J. A. Miller and S. J. Klippenstein, J. Phys. Chem. A **107**, 7783 (2003).
[25] A. D'Anna, A. D'Alessio, and J. Kent, Combust. Sci. Technol. **174**, 279 (2002).
[26] S. J. Klippenstein, L. B. Harding, and Y. Georgievskii, Proc. Combust. Inst. **31**, 221 (2007).
[27] L. Vereecken and J. Peeters, Phys. Chem. Chem. Phys. **5**, 2807 (2003).
[28] C. Cavallotti, D. Polino, A. Frassoldati, and E. Ranzi, J. Phys. Chem. A **116**, 3313 (2012).
[29] H. Wang and M. Frenklach, Combust. Flame **96**, 163 (1994).
[30] H. Wang and M. Frenklach, Combust. Flame **110**, 173 (1997).
[31] G. Blanquart, P. Pepiot-Desjardins, and H. Pitsch, Combust. Flame **156**, 588 (2009).
[32] A. Matsugi and A. Miyoshi, Int. J. Chem. Kinet. **44**, 206 (2012).
[33] E. Goos, A. Burcat, and B. Ruscic, Ideal Gas Thermochemical Database with Updates from Active Thermochemical Tables, ftp://ftp.technion.ac.il/pub/supported/aetdd/thermodunamics (2005).
[34] J. A. Miller, J. P. Senosiain, S. J. Klippenstein, and Y. Georgievskii, J. Phys. Chem. A **112**, 9429 (2008).
[35] Reaction Design, *Chemkin-Pro 15092*, San Diego (2009).
[36] Y. Hidaka, T. Nakamura, A. Miyauchi, T. Shiraishi, and H. Kawano, Int. J. Chem. Kinet. **21**, 643 (1989).
[37] Y. Hidaka, T. Higashihara, N. Ninomiya, H. Masaoka, T. Nakamura, and H. Kawano, Int. J. Chem. Kinet. **28**, 137 (1996).
[38] B. Yang, P. Osswald, Y. Y. Li, J. Wang, L. X. Wei, Z. Y. Tian, F. Qi, and K. Kohse-Höinghaus, Combust. Flame **148**, 198 (2007).
[39] P. Osswald, H. Gldenberg, K. Kohse-Höinghaus, B. Yang, T. Yuan, and F. Qi, Combust. Flame **158**, 2 (2011).
[40] F. Qi, Proc. Combust. Inst. **34**, 33 (2013).

DOI:10.1063/1674-0068/30/cjcp1703031